Article

Activation of CS and CS by ML Complexes

Alireza Ariafard, Nigel J. Brookes, Robert Stranger, and Brian F. Yates

J. Am. Chem. Soc., **2008**, 130 (36), 11928-11938 • DOI: 10.1021/ja800946e • Publication Date (Web): 16 August 2008

JACS
JOURNAL OF THE AMERICAN CHEMICAL SOCIETY

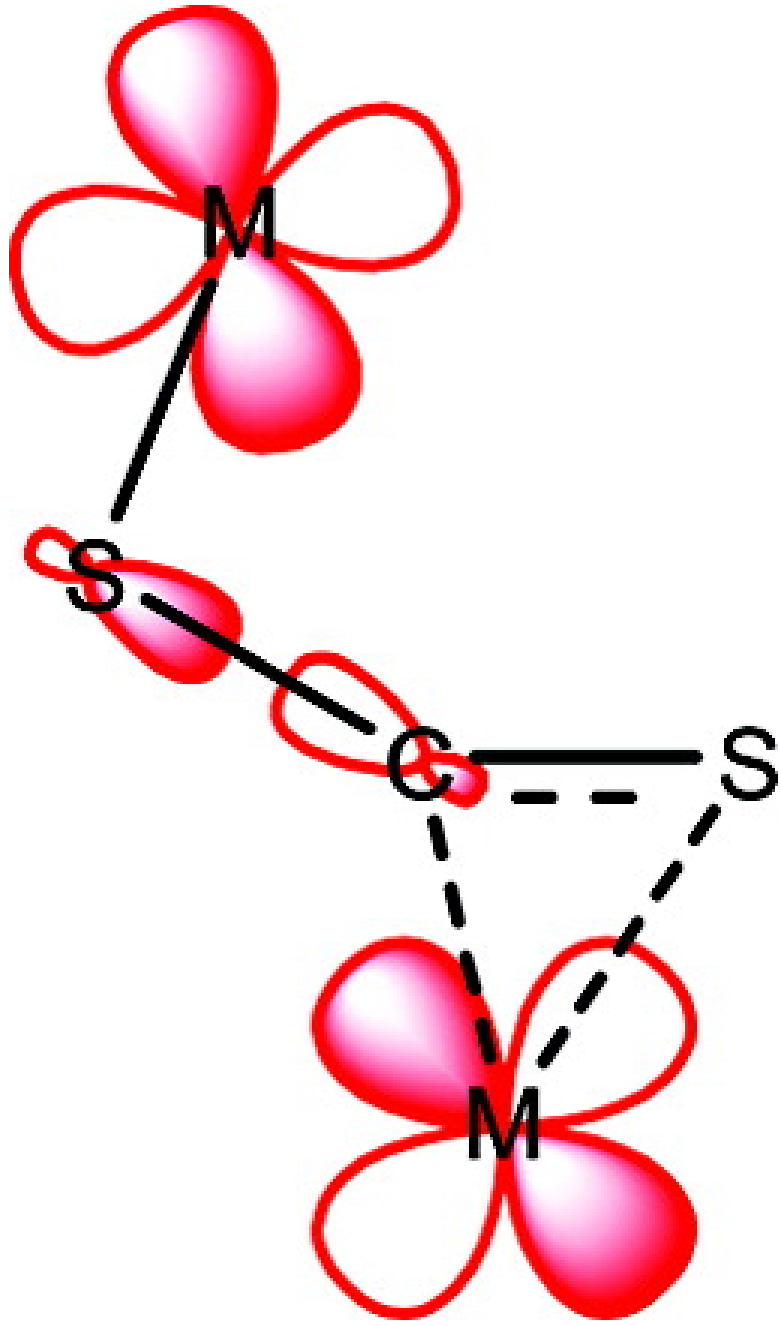

More About This Article

Additional resources and features associated with this article are available within the HTML version:

Journal of the American Chemical Society is published by the American Chemical Society. 1155 Sixteenth Street N.W., Washington, DC 20036

J|A|C|S
ARTICLES

Published on Web 08/16/2008

Activation of CS_2 and CS by ML_3 Complexes

Alireza Ariafard,* Nigel J. Brookes, Robert Stranger, and Brian F. Yates*

School of Chemistry, University of Tasmania, Private Bag 75, Hobart TAS 7001, Australia, and Department of Chemistry, Australian National University, Canberra ACT 0200, Australia

Received February 6, 2008; E-mail: Brian.Yates@utas.edu.au

Abstract: The aim of this study was to determine the best neutral ML_3 metal complexes for activating and cleaving the multiple bonds in CS_2 and CS. Current experimental results show that, so far, only one bond in CS_2 can be cleaved, and that CS can be activated but the bond is not broken. In the work described in this paper, density functional theory calculations have been used to evaluate the effectiveness of different ML_3 complexes to activate the C−S bonds in CS_2 and CS, with M = Mo, Re, W, and Ta and L = NH_2. These calculations show that the combination of Re and Ta in the $L_3Re/CS_2/TaL_3$ complex would be the most promising system for the cleavage of both C−S bonds of CS_2. The reaction to cleave both C−S bonds is predicted to be exothermic by about 700 kJ mol^{-1} and to proceed in an almost barrierless fashion. In addition, we are able to rationalize why the breaking of the C−S bond in CS has not been observed experimentally with M = Mo: this reaction is strongly endothermic. There is a subtle interplay between charge transfer and π back-donation, and it appears that the Mo−C and Mo−S bonds are not strong enough to compensate for the breaking of the C−S bond. Our results suggest that, instead, CS could be cleaved with ReL_3 or, even better, with a combination of ReL_3 and TaL_3. Molecular orbitals and Mulliken charges have been used to help explain these trends and to make predictions about the most promising systems for future experimental exploration.

Introduction

The activation and cleavage of small molecules promoted by three-coordinate early transition metal complexes is one of the challenging subjects of recent research. Of the three-coordinate complexes, the molybdenum complex, $Mo[N(R)Ar]_3$, is commonly used in experimental studies as a catalyst. It is well known, for instance, that this complex cleaves N_2[1–5] to produce $2Mo^{VI}$−N and cleaves SO_2[6] to produce $2Mo^{V}$−O and Mo^{V}−S. This complex is also capable of deoxygenating NO_2, $OSMe_2$, and SO_2[6] and of activating CO,[7,8] NO,[9] and CN^-.[10]

CS_2 has been shown to undergo a variety of reactions with transition metals, including insertion and disproportionation, and there is a growing interest in the activation of CS_2 from catalytic and biological points of view.[11–14] The cleavage of the C−S bonds of CS_2 by $Mo[N(R)Ar]_3$ (R = $C(CD_3)CH_3$ and Ar = 3,5-$C_6H_3Me_2$) has been reported by Cummins and co-workers.[6] They showed that the addition of 1 equiv of CS_2 to $Mo[N(R)Ar]_3$ leads to the formation of $Mo(S)[N(R)Ar]_3$ and (μ-CS)($Mo[N(R)Ar]_3$)$_2$ (eq 1), demonstrating that, although $Mo[N(R)Ar]_3$ is able to break one of the C−S bonds of CS_2, the cleavage of the C−S bond of CS is quite unfeasible. A similar result is also found for the reaction of CS_2 with other transition metal complexes,[15–17] such as [Ru(OEP)] (OEP = octaethylporphyrinato).[16]

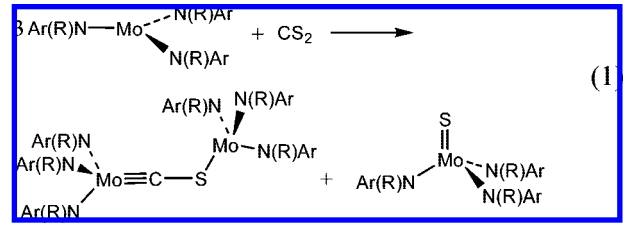

(1)

The most important driving force for the ease of the cleavage of CS_2 versus CS is likely that the C−S bond in CS_2 ($D°_{298}$ =

(1) Laplaza, C. E.; Cummins, C. C. *Science* **1995**, *268*, 861.
(2) Laplaza, C. E.; Johnson, M. J. A.; Peters, J. C.; Odom, A. L.; Kim, E.; Cummins, C. C.; George, G. N.; Pickering, I. J. *J. Am. Chem. Soc.* **1996**, *118*, 8623.
(3) Cummins, C. C. *Chem. Commun.* **1998**, 1777.
(4) Peters, J. C.; Cherry, J. P. F.; Thomas, J. C.; Baraldo, L.; Mindiola, D. J.; Davis, W. M.; Cummins, C. C. *J. Am. Chem. Soc.* **1999**, *121*, 10053.
(5) Gambarotta, S.; Scott, J. *Angew. Chem., Int. Ed.* **2004**, *43*, 5298.
(6) Johnson, A. R.; Davis, W. M.; Cummins, C. C.; Serron, S.; Nolan, S. P.; Musaev, D. G.; Morokuma, K. *J. Am. Chem. Soc.* **1998**, *120*, 2071.
(7) Peters, J. C.; Odom, A. L.; Cummins, C. C. *Chem. Commun.* **1997**, *20*, 1995.
(8) Greco, J. B.; Peters, J. C.; Baker, T. A.; Davis, W. M.; Cummins, C. C.; Wu, G. *J. Am. Chem. Soc.* **2001**, *123*, 5003.
(9) Laplaza, C. E.; Odom, A. L.; Davis, W. M.; Cummins, C. C.; Protasiewicz, J. D. *J. Am. Chem. Soc.* **1995**, *117*, 4999.
(10) Peters, J. C.; Baraldo, L. M.; Baker, T. A.; Johnson, A. R.; Cummins, C. C. *J. Organomet. Chem.* **1999**, *591*, 24.
(11) Butler, I. S.; Fenster, A. E. *J. Organomet. Chem.* **1974**, *66*, 161.
(12) Ibers, J. A. *Chem. Soc. Rev.* **1982**, *11*, 57.
(13) Pandey, K. K. *Coord. Chem. Rev.* **1995**, *140*, 37.
(14) Cheng, P.; Koyanagi, G. K.; Bohme, D. K. *J. Phys. Chem. A* **2006**, *110*, 2718.
(15) Qi, J.-S.; Schrier, P. W.; Fanwick, P. E.; Walton, R. A. *Inorg. Chem.* **1992**, *31*, 258.
(16) Yee, G. T.; Noll, B. C.; Williams, D. K. C.; Sellers, S. P. *Inorg. Chem.* **1997**, *36*, 2904.
(17) Böttcher, H.-C.; Graf, M.; Merzweiler, K.; Wagner, C. *Z. Anorg. Allg. Chem.* **2001**, *627*, 2657.

10.1021/ja800946e CCC: $40.75

430.5 ± 13 kJ mol^{-1}) is much weaker than in CS ($D°_{298}$ = 714.1 ± 1.2 kJ mol^{-1}).[18] In contrast, as mentioned above, Mo[N(R)Ar]$_3$ is able to cleave the N−N bond of N_2, which is approximately 240 kJ mol^{-1} stronger than the C−S bond of CS, due to the formation of a very strong Mo−N bond. This implies that, for the case of CS, the molybdenum complex is not properly chosen to form thermodynamically optimized M−C or M−S bonds.

Recently, based on theoretical studies, a new approach for cleaving CN^- [19] and CO[20,21] by neutral model complexes M[NH$_2$]$_3$ has been introduced. In these studies, the metal center M was chosen such that it gives the strongest M−L bonds in the product, providing a thermodynamic driving force for the cleavage reactions. The results of a systematic study by Christian et al. on the bonding properties of neutral L−M[NH$_2$]$_3$ complexes showed that M = Re, W, and Ta form the strongest bonds with L = C, N, and O, respectively.[22] Therefore, it was predicted that the combination of Re[NH$_3$]$_3$ and Ta[NH$_3$]$_3$ is best suited to breaking CO, while the combination of Re[NH$_2$]$_3$ and W[NH$_2$]$_3$ is best suited to breaking CN^-.

To date, the mechanism of cleavage of N_2,[4,23–30] N_2O,[31,32] CO,[7,8,20,21] and CN^- [10,19] by three-coordinate complexes has been well studied. However, an in-depth understanding of the mechanism of molybdenum-promoted CS_2 cleavage reaction is still lacking. In this study, we attempt to provide a possible mechanism with the aid of B3LYP density functional theory (DFT) calculations, aimed at rationalizing why the cleavage of the C−S bond of CS is not observed experimentally. We also wish to investigate theoretically which metal gives the strongest M−S bond and to design promising catalysts capable of cleaving both C−S bonds of CS_2.

Computational Details

GAUSSIAN 03[33] was used to fully optimize all the structures reported in this paper at the B3LYP[34–36] level of density functional theory. The effective core potentials of Hay and Wadt with double-ζ valence basis sets (LANL2DZ)[37,38] were chosen to describe the transition metals. The 6-31G(d)[39] basis set was used for other atoms. This basis set combination will be referred to as BS1. Frequency calculations at the same level of theory have also been performed to identify all of the stationary points as minima (zero imaginary frequencies) or transition structures (one imaginary frequency).

To test the accuracy of the medium-size basis set (BS1) used, we carried out single-point energy calculations for all structures by using a larger basis set, the LANL2augmented:6-311+G(2d,p) basis set, incorporating the LANL2 effective core potential, a large LANL2TZ+(3f) basis set on the transition metals (see Supporting Information), and the 6-311+G(2d,p) basis set on other atoms. This basis set will be referred to as BS2. In the energy profile shown in Figures 1 and 8–11 (below), we used the B3LYP/BS2//B3LYP/BS1 energies.

We further performed single-point CCSD(T)/BS1 calculations for several selected structures based on the B3LYP/BS1-optimized structures to test the effect of the electron correlation. The results show that the change in the relative energy is small (see Table A in the Supporting Information for more details).

Natural bond orbital (NBO)[40] analysis was employed to evaluate the electron population. Mulliken population analyses were carried out using the MullPop program.[41]

Results and Discussion

MoL_3 + CS_2 and MoL_3 + CS. As mentioned in the Introduction, we shall here investigate the mechanism of eq 1 and show why Mo[N(R)Ar]$_3$ is not capable of breaking CS to yield Mo(S)[N(R)Ar]$_3$ and Mo(C)[N(R)Ar]$_3$. To understand this, we used the model reactant complex Mo(NH$_2$)$_3$[42] in these calculations, as was used previously.[19–22,25,28,29,43] The overall reaction profile, showing the relative energies of the reactants, intermediates, and products for the reaction given in eq 1, is plotted in Figure 1. **N_X** and **NTS_X** are the nomenclatures used for the species on the potential energy surface (PES), where **X = S** stands for singlet, **X = D** for doublet, **X = T** for triplet, and **X = Q** for quartet spin states. **N** represents the minimum structures, and **NTS** corresponds to the transition structures on the B3LYP PES.

In accordance with the earlier studies, the quartet state of Mo(NH$_2$)$_3$ (**1_Q**) is calculated to be more stable than the doublet state, **1_D**, by about 59.8 kJ mol^{-1}. The first step of reaction 1 is surmised to be coordination of CS_2 to Mo(NH$_2$)$_3$. The CS_2 in singlet ground state binds to Mo via an η^2-side-on coordination and gives **2_D** with an energy drop of 110.6 kJ mol^{-1}. **2_D**, having a doublet state, is about 114.0 kJ mol^{-1} more stable than **2_Q**, having a quartet state. The barrier height for the **1_Q** + CS_2 → **2_Q** reaction is calculated to be 29.7 kJ mol^{-1}. As can be seen from Figure 2, the Mo−C and Mo−S1 bond distances in **2_D** are found to be about 0.262 and 0.199 Å shorter than in **2_Q**, respectively, indicating that the Mo−CS_2 bonding

(18) Lide, D. R. *CRC Handbook of Chemistry and Physics*, 84th ed.; CRC Press: Boca Raton, FL, 2004.
(19) Christian, G.; Stranger, R.; Yates, B. F.; Cummins, C. C. *Dalton Trans.* **2008**, 338.
(20) Christian, G.; Stranger, R.; Yates, B. F.; Cummins, C. C. *Eur. J. Inorg. Chem.* **2007**, 3736.
(21) Christian, G.; Stranger.; Petrie, S.; R.; Yates, B. F.; Cummins, C. C. *Chem. Eur. J.* **2007**, *13*, 4246.
(22) Christian, G.; Stranger, R.; Yates, B. F. *Inorg. Chem.* **2006**, *45*, 6851.
(23) Mindiola, D. J.; Meyer, K.; Cherry, J.-P. F.; Baker, T. A.; Cummins, C. C. *Organometallics* **2000**, *19*, 1622.
(24) Tsai, Y. C.; Cummins, C. C. *Inorg. Chim. Acta* **2003**, *345*, 63.
(25) Cui, Q.; Musaev, D. G.; Svensson, M.; Sieber, S.; Morokuma, K. *J. Am. Chem. Soc.* **1995**, *117*, 12366.
(26) Neyman, K. M.; Nasluzov, V. A.; Hahn, J.; Landis, C. R.; Rösch, N. *Organometallics* **1997**, *16*, 995.
(27) Hahn, J.; Landis, C. R.; Nasluzov, V. A.; Neyman, K. M.; Rösch, N. *Inorg. Chem.* **1997**, *36*, 3947.
(28) Christian, G.; Driver, J.; Stranger, R. *Faraday Discuss.* **2003**, *124*, 331.
(29) Christian, G.; Stranger, R. *Dalton Trans.* **2004**, 2492.
(30) Christian, G.; Stranger, R.; Yates, B. F.; Graham, D. C. *Dalton Trans.* **2005**, 962.
(31) Khoroshun, D. V.; Musaev, D. G.; Morokuma, K. *Organometallics* **1999**, *18*, 5653.
(32) Cherry, J.-P. F.; Johnson, A. R.; Baraldo, L. M.; Tsai, Y.-C.; Cummins, C. C.; Kryatov, S. V.; Rybak-Akimova, E. V.; Capps, K. B.; Hoff, C. D.; Haar, C. M.; Nolan, S. P. *J. Am. Chem. Soc.* **2001**, *123*, 7271.
(33) Frisch, M. J.; et al. *Gaussian 03*, revision D01; Gaussian, Inc.: Pittsburgh, PA, 2003.
(34) Becke, A. D. *J. Chem. Phys.* **1993**, *98*, 5648.
(35) Lee, C.; Yang, W.; Parr, R. G. *Phys. Rev. B* **1988**, *37*, 785.
(36) Stephens, P. J.; Devlin, F. J.; Chabalowski, C. F. *J. Phys. Chem.* **1994**, *98*, 11623.
(37) Wadt, W. R.; Hay, P. J. *J. Chem. Phys.* **1985**, *82*, 284.
(38) Hay, P. J.; Wadt, W. R. *J. Chem. Phys.* **1985**, *82*, 299.
(39) Hariharan, P. C.; Pople, J. A. *Theor. Chim. Acta* **1973**, *28*, 213.
(40) Glendening, E. D.; Read, A. E.; Carpenter, J. E.; Weinhold, F. *NBO*, version 3.1; Gaussian, Inc.: Pittsburgh, PA, 2003.
(41) Pis Diez, R. *MullPop*; National University of La Plata: La Plata, Argentina; 2003.
(42) To study the steric effect missed by the small model calculations, we performed B3LYP/BS1 optimizations on the mechanism of CS breaking promoted by the more realistic [N(*i*-Pr)Ph]$_3$M/CS/M′[N(*i*-Pr)Ph]$_3$ systems (see Table B in the Supporting Information for the detailed results). The calculation results show that the extra bulkiness of the ancillary ligands does not affect our conclusions made on the basis of the small NH$_2$ model.
(43) Graham, D. C.; Beran, G. J. O.; Head-Gordon, M.; Christian, G.; Stranger, R.; Yates, B. F. *J. Phys. Chem. A* **2005**, *109*, 6762.

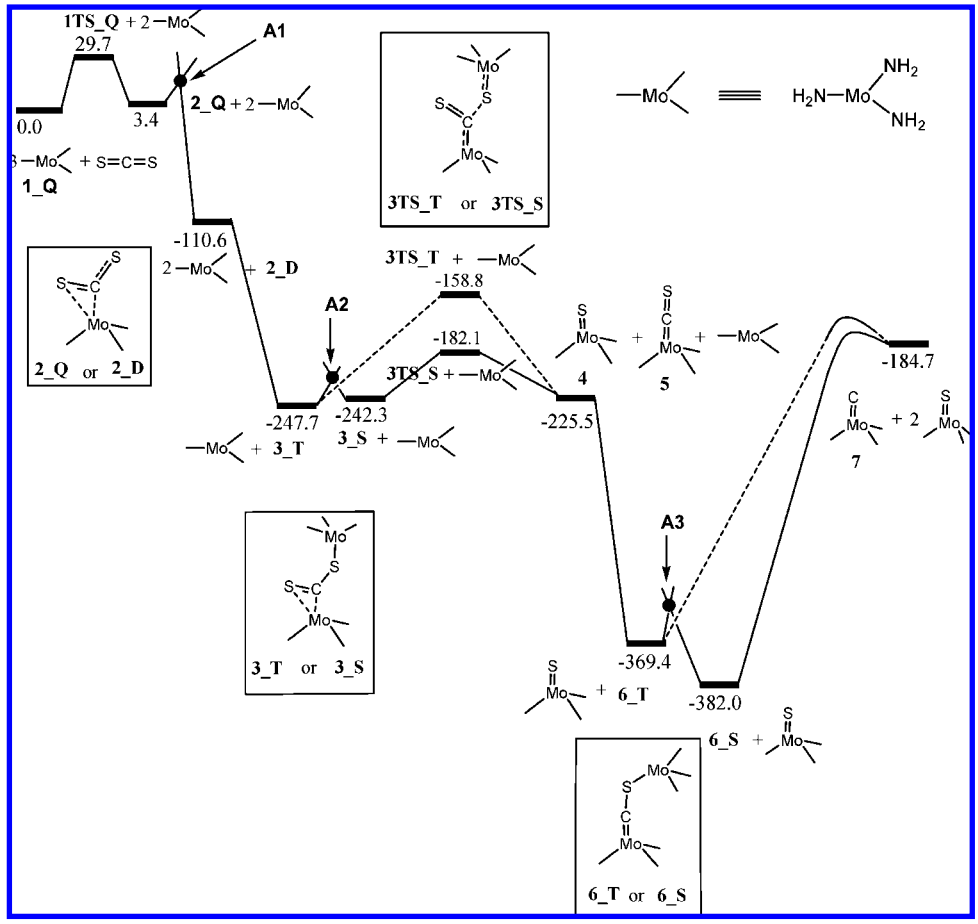

Figure 1. Potential energy surface for the reaction $3Mo(NH_2)_3 + CS_2$.

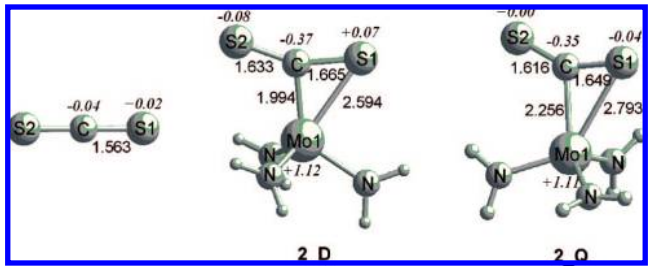

Figure 2. Geometries and Mulliken charges for species involved in the initial coordination of $Mo(NH_2)_3$ to CS_2.

interaction in **2_D** is stronger than in **2_Q**. In this coordination mode, CS_2 appears to be a very good π-acid ligand, as judged from the substantial lengthening of the C−S bond distances in **2_D** and **2_Q** compared to those in the free CS_2 molecule (Figure 2). The Mulliken charge distribution calculated for CS_2, **2_D**, and **2_Q** further supports the argument here. It follows from Figure 2 that the electron population of CS_2 increases from 0.0 in the free CS_2 molecule to −0.38 in **2_D** and −0.39 in **2_Q**, suggesting that π-back-donation plays a crucial role in the Mo−CS_2 bonding interaction. The η^1-S end-on coordination of CS_2 does not correspond to a minimum on the PES of the doublet state, and all attempts led to **2_D**. This result is consistent with the earlier findings that the η^1-S end-on coordination of CS_2 is unfavorable for the metals that are susceptible to π-back-donation.[44]

A qualitative evaluation of the molecular orbitals allows us to understand the causes of the differences in the CS_2 binding energies between **2_D** and **2_Q**. Figure 3a shows schematically the π orbitals for CS_2. Of the four occupied π orbitals, only π_1 and π_2, corresponding to the symmetry-adapted orbitals, act as donor orbitals (Figure 3b). Our calculated wave functions show that the d_{yz} orbital of $Mo[NH_2]_3$ is stabilized through its interaction with π_3. For **2_D**, the major contribution to the singly occupied highest occupied molecular orbital (HOMO) is from a bonding interaction between the d_{xz} orbital of $Mo[NH_2]_3$ and the π_3' of CS_2. For **2_Q**, one of the electrons occupies the $1\sigma^*$ antibonding orbital, weakening the Mo−CS_2 bonding. This could explain why **2_D** is more stable than **2_Q**.

Since $[NH_2]_3Mo$ has a quartet spin ground state and CS_2 a singlet state, the reaction begins on the quartet surface. To reach the doublet encounter complex **2_D**, an intersystem crossing occurs at the minimum energy crossing point (MECP). The MECP, **A1**, was located with the code of Harvey[45,46] at the B3LYP level of theory with the BS1 basis set (Figure 4). **A1** is calculated to lie only 0.08 kJ mol^{-1} higher than **2_Q** (at the B3LYP/BS1 level). These results suggest that the formation of **2_D** is a feasible process.

The next step of the reaction is expected to be coordination of the second fragment **1_Q** to **2_D**. A dinuclear intermediate with a triplet state (**3_T**, Figure 5) should be produced via the process because the ground states of **1_Q** and **2_D** are quartet

(44) Schenk, W. A.; Schwletzke, T. *Organometallics* **1983**, *2*, 1905.
(45) Harvey, J. N.; Aschi, M.; Schwarz, H.; Koch, W. *Theor. Chem. Acc.* **1998**, *99*, 95.
(46) Harvey, J. N.; Aschi, M. *Phys. Chem. Chem. Phys.* **1999**, *1*, 5555.

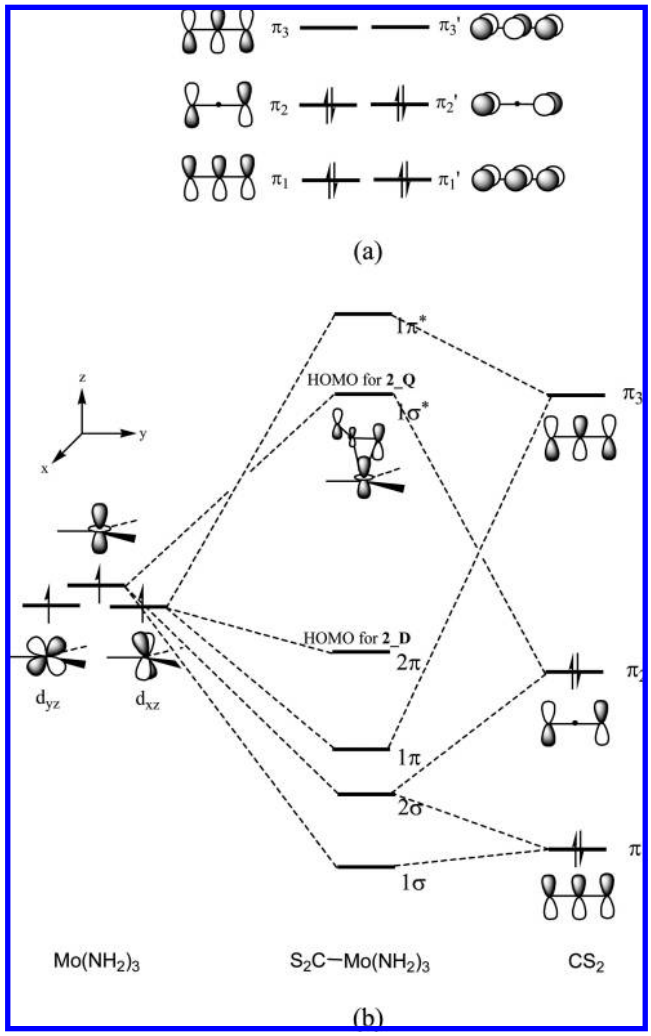

Figure 3. Molecular orbital diagram for the coordination of $Mo(NH_2)_3$ to CS_2.

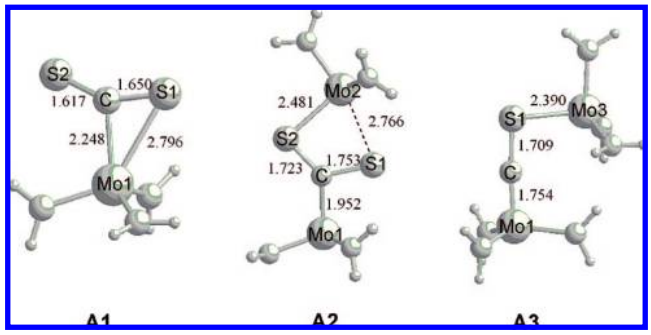

Figure 4. Geometries for the minimum energy crossing points corresponding to Figure 1.

and doublet, respectively. The reaction **1_Q** + **2_D** → **3_T** proceeds in a barrierless fashion and is found to be exothermic by 137.1 kJ mol^{-1}. The singlet state of the binuclear complex $[NH_2]_3Mo-CS_2-Mo[NH_2]_3$ (**3_S**) is about 5.4 kJ mol^{-1} higher in energy than the corresponding triplet-state complex. **3_T** can be converted to the less stable intermediate **3_S** via an intersystem crossing. The result obtained from the location of the MECP, **A2**, shows that the spin crossover barrier to the formation of **3_S** is approximately 6.0 kJ mol^{-1} (at the B3LYP/BS1 level, Figure 4). A comparison of the geometries of the

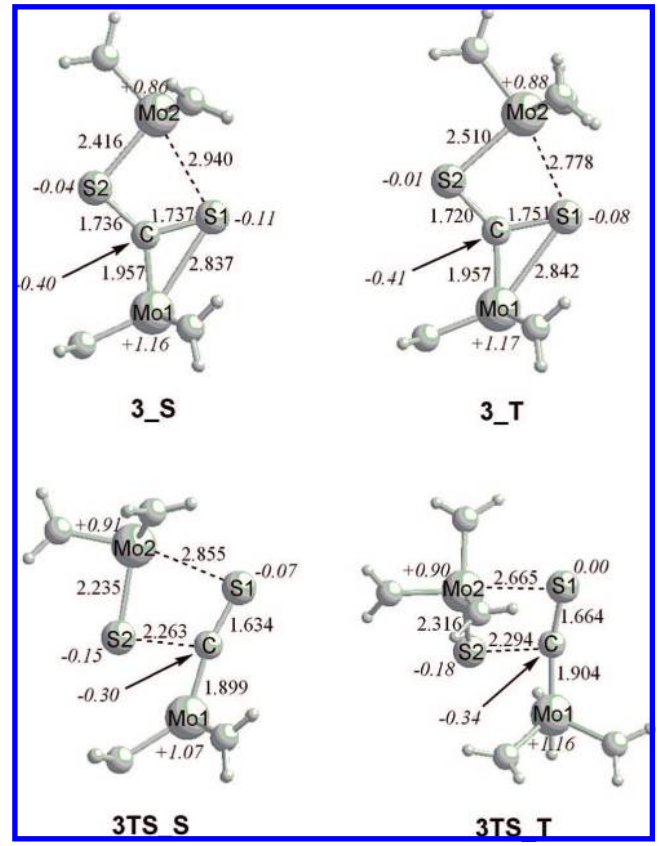

Figure 5. Geometries and Mulliken charges for species involved in breaking the first C−S bond.

resting-state complexes **2_D** and **3_S** reveals that CS_2 in **3_S** is more activated than in **2_D**. The C−S1 and C−S2 bond distances are elongated from 1.665 and 1.663 Å in **2_D** to 1.737 and 1.736 Å in **3_S**. The Mo1−C bond is shortened from 1.994 Å in **2_D** to 1.957 Å in **3_S**. The charge carried by CS_2 in **3_S** (−0.55) is more negative than in **2_D** (−0.38). These results imply that the charge transfer from the metal fragments to CS_2 in **3_S** is more significant. The calculations also indicate that the metal fragment $Mo1[NH_2]_3$ (+0.42) in **3_S** is much more positively charged than $Mo2(NH_2)_3$ (+0.13), suggesting that the contribution of $Mo1(NH_2)_3$ to metal → CS_2 back-donation is significantly larger. This idea also finds support from the results of the NBO population analysis. In **3_S**, the d_{xz} and d_{yz} orbitals of both Mo1 and Mo2 participate in the π-back-donation interaction, the population of which for Mo1 (2.16e) is calculated to be smaller than for Mo2 (2.53e).

The cleavage of one of the C−S bonds of CS_2 can take place through both of the intermediates **3_T** and **3_S** and through the transition structures **3TS_T** and **3TS_S** to form the $[NH_2]_3MoS$ (**4**) and $[NH_2]_3MoCS$ (**5**) products in the doublet spin states. The reaction is predicted to be endothermic with respect to both intermediates **3_T** and **3_S**. Both transition states involve the breaking of the C−S2 bond and the formation of a new C−S1 π bond. For example, in **3TS_S**, the C−S2 bond (2.263 Å) is longer and the C−S1 bond (1.634 Å) is shorter than the corresponding bonds (1.736 and 1.751 Å, respectively) in **3_S**. In the transition structure **3TS_T**, Mo2 is substantially out of the S1−C−Mo1 plane, while **3TS_S** adopts a structure with a coplanar orientation of the Mo2−S2−C plane with respect to the Mo1−S1−C plane. The C−S2 distance in the triplet transition structure **3TS_T** is 0.031 Å longer than in the

Scheme 1

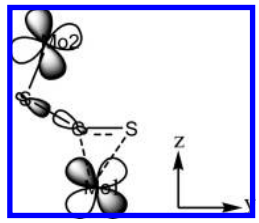

singlet. This result points to a late transition state for **3TS_T** compared to **3TS_S**, consistent with the observation that **3TS_T** lies higher in energy than singlet **3TS_S** by 23.3 kJ mol^{-1}. From this result, one may conclude that the C−S bond cleavage of CS_2 through the singlet surface should be kinetically favored over the process through the triplet.

Of the d_{yz} orbitals having the appropriate symmetry for interaction with σ^*_{C-S2} (Scheme 1), the Mo2 d_{yz} orbital, which corresponds to HOMO in **3_S** and HOMO−1 in **3_T**, is more available for this interaction. The Mo1 d_{yz} orbital, which is mainly stabilized by the Mo1→ CS_2 back-donation interaction, has a negligible contribution to the bond-breaking process. Upon going from **3_S** to **3TS_S**, the σ^*_{C-S2} orbital overlaps well with the doubly occupied d_{yz} orbital of Mo2 and gives the planar transition-state structure for **3TS_S**. On the other hand, the singly occupied d_{yz} orbital of Mo2 in the triplet state surface has one electron short of the configuration necessary to cleave the C−S2 bond. As a result, the $[NH_2]_3$Mo2 is displaced out of the S1−C−Mo1 plane to provide a bonding interaction between lower-lying occupied orbitals and σ^*_{C-S2}, leading to the nonplanarity and instability found in the transition state **3TS_T**.

Once the cleavage process has completed, the reaction further proceeds via coordination of $[NH_2]_3$MoCS to a third Mo$[NH_2]_3$ complex. The triplet complex **6_T** is expected to be the product of the coordination reaction because the ground states for $[NH_2]_3$MoCS and Mo$[NH_2]_3$ are doublet and quartet, respectively. The overall reaction Mo$[NH_2]_3$ + **5** → **6_T** is predicted to be strongly exothermic by 144 kJ mol^{-1} and has no barrier. A spin crossover is required to form the singlet intermediate **6_S**, which is 12.6 kJ mol^{-1} more stable than its triplet analogue. To estimate the activation energy for the spin crossing process, the MECP, **A3**, was identified by using the method of Harvey et al.[45,46] as mentioned above (Figure 4). The calculations show that the spin crossover occurs with a barrier of 10.7 kJ mol^{-1} at the B3LYP/BS1 level of theory. The result that **6_S** is more stable than **6_T** agrees well with the experimental findings that the dinuclear intermediate [N(R)Ar]$_3$MoCSMo[N(R)Ar] is diamagnetic.[6] The selected calculated bond distances for the model complex **6_S** are in fairly good agreement with their experimental values (in parentheses, Figure 6).

The C−S bond distances in **6_S** and **6_T** are about 0.1 Å longer than in **5**, and the total charges on CS in **6_S** (−0.326) and **6_T** (−0.308) are more negative than in **5** (−0.291) (Figure 6). These results imply that the Mo-to-CS back-donation in the dinuclear intermediates is considerably stronger than in **5**. The calculations also show that, in agreement with the experimental observations,[6] the Mo3−S−C angle (103.5°) in **6_S** is bent, whereas the Mo1−C−S angle (174.9°) is roughly linear. This result is in contrast to the situation in the dinitrogen intermediates $[NH_2]_3$Mo−N_2−Mo$[NH_2]_3$, where both of the Mo−N−N angles are nearly linear. The singlet linear conformer **6a_S**, in which the Mo3−S−C angle was kept fixed at 180°, is calculated to be 116.6 kJ mol^{-1} higher in energy than **6_S**. The driving

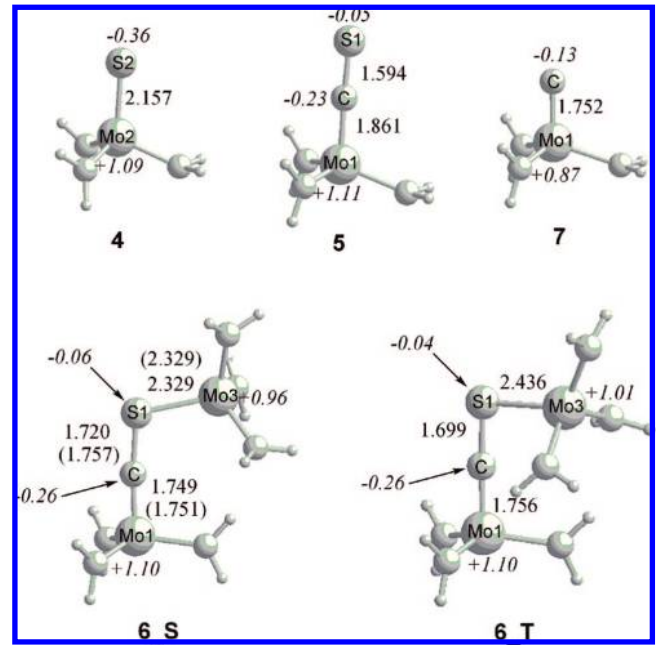

Figure 6. Geometries and Mulliken charges for products of the reaction $3Mo(NH_2)_3 + CS_2$. (Experimental values in parentheses.)

force toward the nonlinearity in **6_S** is most likely a result of the weak π-donor properties of Mo3 and strongly double-faced (i.e., having perpendicular π orbitals) π-donor properties of Mo1. In contrast to the bonding characteristic in **6_S**, both of the Mo metal centers in $[NH_2]_3$Mo−N_2−Mo$[NH_2]_3$ act as double-face π-donors with perpendicular π orbitals and simultaneously interact with both of the N_2 π-antibonding orbitals. This electronic feature provides a strong driving force toward linearity for the Mo−N−N−Mo linkage. Further support for the claim can also be found from the study of the frontier molecular orbitals of the singlet forms of $[NH_2]_3$Mo−N_2−Mo$[NH_2]_3$ and $[NH_2]_3$Mo−CS−Mo$[NH_2]_3$ (Chart 1). **MO1** and **MO2** are the orbitals derived from the bonding interactions between N_2 π-antibonding orbitals and the antisymmetric combination of d_π orbitals on the Mo atoms (Chart 1a). The symmetric combination of d_π orbitals on the Mo atoms is destabilized as a result of the repulsive interaction with the N_2 π-bonding orbitals (**MO3** and **MO4**). The percentage contribution of Mo1 (Mo2) in **MO1** and **MO2** is 33% (33%) and 22% (22%), respectively, indicating that the contributions of the Mo1 and Mo2 d_π orbitals to the π-bonding interactions in $[NH_2]_3$-Mo1−N_2−Mo2$[NH_2]_3$ are the same and significant (Chart 1a). In contrast, there is very little contribution from the Mo3 d_π orbitals to the π-bonding orbitals (**MO1′** and **MO2′**) of **6a_S** (Chart 1b). This result substantiates the notion that the Mo3-to-CS back-donation contribution to the Mo−CS−Mo π-bonding interactions is negligible. In such a case, a linear geometry suffers from the Mo3−S π-antibonding interaction shown in **MO3′**. Thus, the Mo3−S−C angle decreases from 180° in **6a_S** to 103° in **6_S** to turn off the antibonding interaction. In addition, since the S-to-Mo3 σ-donation is the dominating bonding mode, the empty d_σ orbital of Mo3 preferentially interacts with the higher lying π1 orbital of $(NH_2)_3$MoCS rather than its lower lying σ orbital (see **MO1″** and Chart 1c), leading to the formation of bent intermediate **6_S**.

Our calculations, in reasonable agreement with experimental findings,[6] predict a pseudo-C_3 symmetry around the Mo1 center and a pseudo-C_s symmetry around the Mo3 center. This means

Chart 1. Comparison of the Molecular Orbitals in $(NH_2)_3Mo-N=N-Mo(NH_2)_3$ and $(NH_2)_3Mo'C-S-Mo(NH_2)_3$

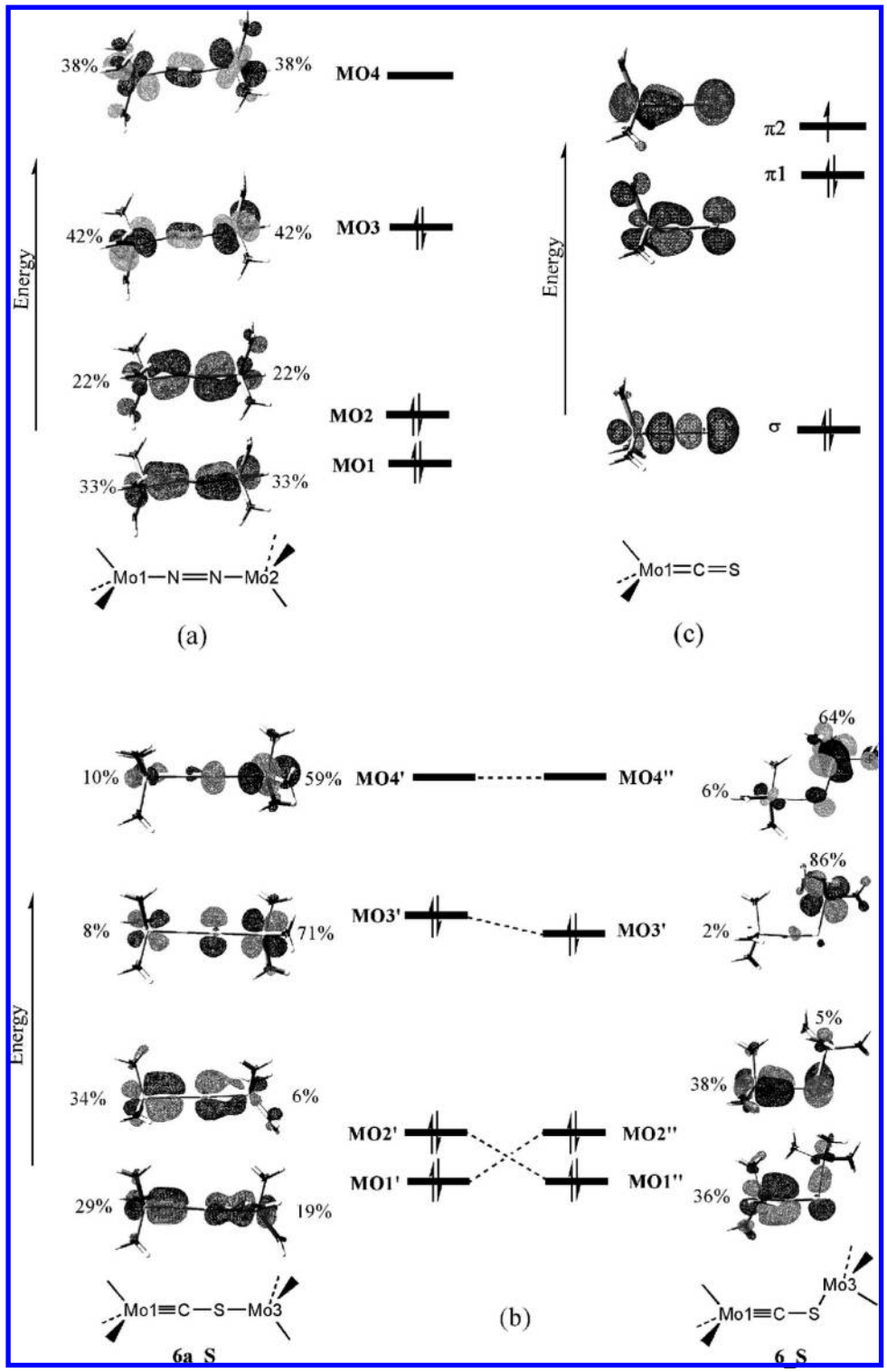

that the ligand rotation only happens for one of the amide ligands of Mo3. In a recent study, we explored computationally in detail the structure and bonding of $[NH_2]_3Mo-N_2-Mo[NH_2]_3$ and showed that the lone pair on the rotated amide ligands is capable of interacting with the empty **MO4** orbital, giving rise to the higher stability of the singlet form relative to its triplet analogue.[47] It is expected that, in such an intermediate, the ligand rotation occurs at each metal center because the percentage contribution of Mo1 and Mo2 to **MO4** is the same and significant (38%). In contrast, for **6_S**, the percentage contribution of the Mo3 d_π orbital (64%) to **MO4″** is much higher than that of the Mo1 d_π orbital (6%). This imbalance in orbital size causes one amide group on Mo3 to rotate by 90°, while no rotation is observed on Mo1. Indeed, the imbalance comes from the fact that the π back-donation interactions mainly occur from

(47) Ariafard, A.; Brookes, N. J.; Stranger, R.; Yates, B. F. *Chem. Eur. J.* **2008**, *14*, 6119–6124.

Scheme 2

$$E(\text{M}-\text{S}) = E[(\text{NH}_2)_3\text{M}-\text{S}] - E[\text{S}] - E[\text{M}(\text{NH}_2)_3]$$

M	Mo	Nb	Hf	Ta	W	Re
E(M−S) (kJ/mol)	428.4	543.4	378.2	595.3	500.3	435.3

the d_π orbitals of Mo1 to CS. This electronic feature increases the Mo1 d_π orbital components and decreases the Mo3 d_π orbital components in **MO1″** and **MO2″**, leaving the minimum Mo1 d_π orbital component and the maximum Mo3 d_π orbital component in **MO3″** and **MO4″**.

Finally, we wish to point out that, although the dinuclear intermediates possess the required number of electrons to reductively cleave the C−S bond, the conversion of **6_S** (or **6_T**) to **4** + **7** is thermodynamically unfavorable because it is a highly endothermic process. This result is consistent with the experimental observation that $[N(R)Ar]_3MoCSMo[N(R)Ar]$ and $[N(R)Ar]_3MoS$ are the only species formed when $[N(R)Ar]_3Mo$ is treated with CS_2.[6] The endothermicity of the step can be rationalized from the notion that the Mo−C and Mo−S bonds are not strong enough to provide the thermodynamic driving force for the cleavage of CS.

M−S Bonds. In an earlier work,[22] we showed that, for neutral $[NH_2]_3M-C$ complexes, the strongest M−C bond occurs for M = Re with d^4 configuration. The Re^{III}−C bond was calculated to be 207 kJ mol^{-1} stronger than the Mo^{III}−C bond. To determine which metal gives the strongest M−S bond, we calculated the M^{III}−S (M = Hf, Ta, Mo, W, Re) bond strengths using the equation shown in Scheme 2, where the B3LYP/BS2//B3LYP/BS1 calculations were used. The results of the calculations show that the M−S bond strength follows the order M = Hf < Mo < Re < W < Nb < Ta, with the Ta−S bond being about 171 kJ mol^{-1} stronger than the Mo−S bond. The W−S bond is calculated to be stronger than the Mo−S bond and the Ta−S bond stronger than the Nb−S bond. These results are consistent with those obtained for other $[NH_2]_3M-L$ systems,[22] where the M−L bond strength increases down a group. This trend was rationalized in terms of the more diffuse d orbitals of higher period transition metals, resulting in enhanced metal−ligand interaction.

The trend that the M−S bond strength increases in the order M = Hf < Re < W < Ta can be explained partly by the molecular orbital diagram shown in Figure 7. For $[NH_2]_3TaS$, the singly occupied orbitals of sulfur (p_z and p_x) interact with the d_{z^2} and d_{xz} metal orbitals, yielding the bonding and antibonding orbitals 1σ, 1π, 1σ*, and 1π*. The doubly occupied p_y orbital of sulfur can also interact with the unoccupied d_{yz} orbital of tantalum, yielding the bonding and antibonding orbitals 2π and 2π *. Since Re (or W) has two (or one) electrons more than Ta, the antibonding orbital 2π* shown in Figure 7 is fully (or partially) occupied, weakening the M−S bond. For M = Hf, the bonding orbital 2π is singly occupied, resulting in the weaker Hf−S bond compared to the Ta−S bond.

Another reason for the stronger Ta−S bond compared to W−S and Re−S can be explained as follows. During the course of the reaction of $[NH_2]_3M + S \rightarrow [NH_2]_3MS$, the oxidation state of M changes from M^{III} to M^{V}. The ionization potential based on the equation $[NH_2]_3M \rightarrow [NH_2]_3M^{2+} + 2e$ is calculated to be 19.6, 18.4, and 17.6 eV for M = Re, W, and Ta, respectively. Thus, it is predicted that $[NH_2]_3Ta$ is capable of losing two electrons much more easily than its W and Re analogues. These results suggest that M = Ta is intrinsically more susceptible than M = W and Re to the formation of the complex $[NH_2]_3MS$.

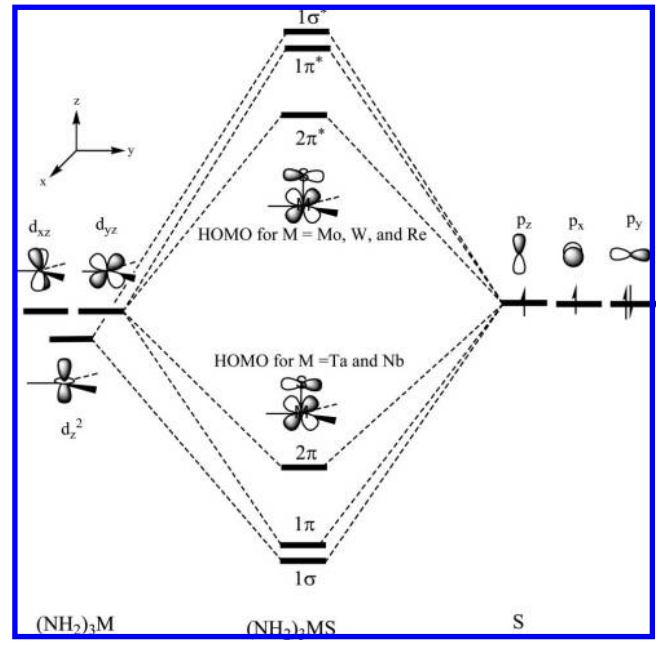

Figure 7. Molecular orbital diagram for coordination of sulfur to the metal fragment.

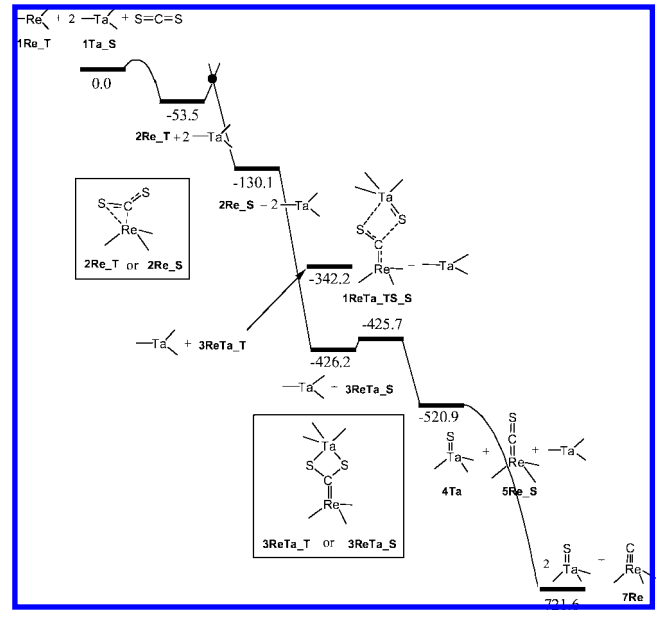

Figure 8. Potential energy surface for the reaction $Re(NH_2)_3 + CS_2 + 2Ta(NH_2)_3$.

Activation of CS_2. On the basis of these results, one may predict that a mixed-metal system involving $[N(R)Ar]_3Re/CS_2/Ta[N(R)Ar]_3$ and $[N(R)Ar]_3Re/CS/Ta[N(R)Ar]_3$ is best suited to cleaving both C−S bonds of CS_2; in this system, the reaction conditions should be adjusted in such a way that CS_2 (or CS) binds to $[N(R)Ar]_3Re$ through carbon and to $[N(R)Ar]_3Ta$ through sulfur.[48] Accordingly, we extended the study of CS_2 cleavage reaction to the $[NH_2]_3Re/CS_2/Ta[NH_2]_3$ system to

(48) There is, of course, the possibility that the mixed-metal systems may not work because of reasons not considered in the calculations, such as unexpected side reactions.

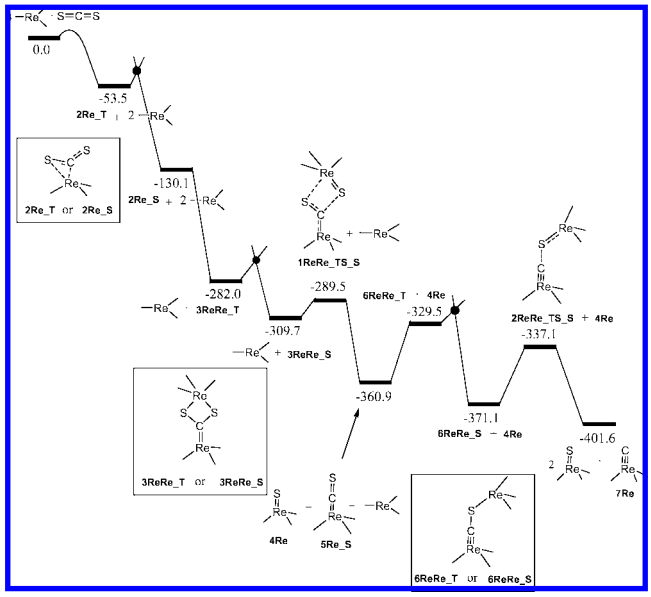

Figure 9. Potential energy surface for the reaction $3Re(NH_2)_3 + CS_2$.

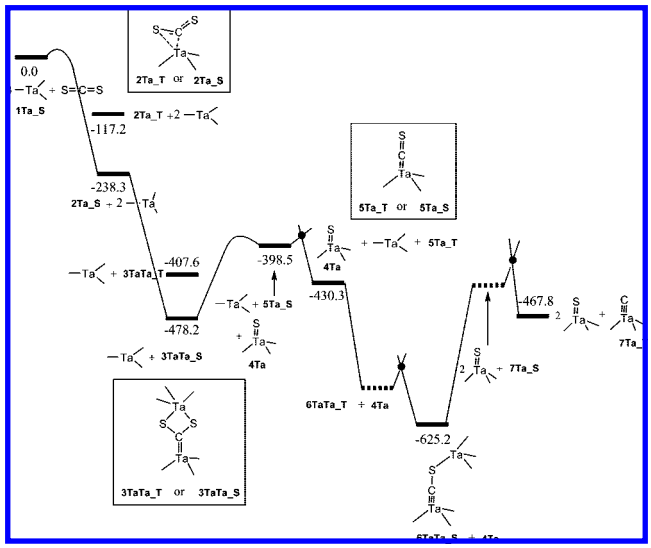

Figure 10. Potential energy surface for the reaction $3Ta(NH_2)_3 + CS_2$.

assess the effect of the mixed-metal fragments on the mechanism and energetics of the reaction. The calculations were also carried out on $[NH_2]_3Re/CS_2/Re[NH_2]_3$, $[NH_2]_3Ta/CS_2/Ta[NH_2]_3$, and $[NH_2]_3Ta/CS_2/Re[NH_2]_3$ systems for the purpose of comparison. Energy profiles of the CS_2 cleavage reaction brought about by the mixed-metal systems are compared in Figures 8–11. It follows from such a comparison that the $[NH_2]_3Re/CS_2/Ta[NH_2]_3$ system is, as expected, the most promising approach to CS_2 cleavage. The reaction **3ReTa_S** → **4Ta** + **5Re_S** is exothermic by 94.7 kJ mol^{-1} and has a barrier of only 0.5 kJ mol^{-1}. In addition, the reaction **5Re_S** + **1Ta_S** → **4Ta** + **7Re** is even more exothermic, with $\Delta E = 200.7$ kJ mol^{-1}, and proceeds in a barrierless fashion.

In agreement with findings from previous studies, the ground-state configurations for $Re(NH_2)_3$ and $Ta(NH_2)_3$ are calculated to be triplet and singlet, respectively. The reaction of $Re(NH_2)_3$ with CS_2 gives the singlet ground state **2Re_S**, preceded by a spin flip from the triplet to the singlet state (Figures 8 and 9). It is expected that, due to the occupancy of the Re−CS_2 σ^* antibonding orbital, the triplet state of $(NH_2)_3Re-CS_2$ (**2Re_T**)

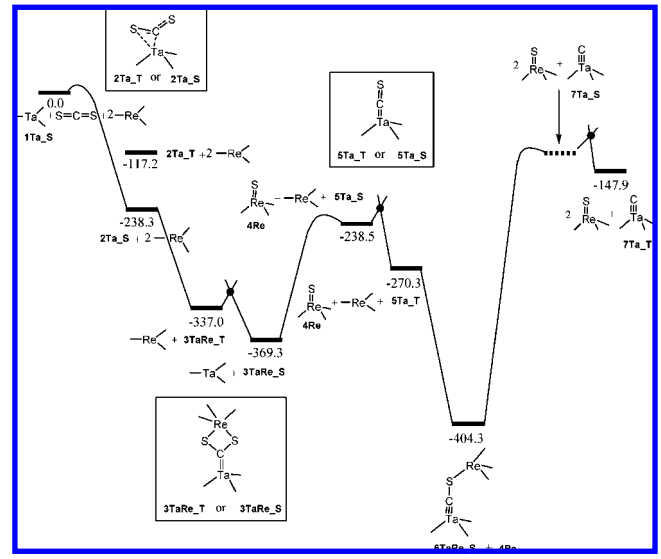

Figure 11. Potential energy surface for the reaction $Ta(NH_2)_3 + CS_2 + 2Re(NH_2)_3$.

is less stable than **2Re_S**. The **2Ta_S** with singlet spin state is formed upon coordination of CS_2 to $Ta(NH_2)_3$ (Figure 10). The triplet state of $(NH_2)_3Ta-CS_2$ (**2Ta_T**) is calculated to be less stable than **2Ta_S** by 121.1 kJ mol^{-1}. The CS_2 binds 108.2 kJ mol^{-1} more strongly to $Ta(NH_2)_3$ than to $Re(NH_2)_3$. This result is in contrast to the previous findings that the binding of CO to $Re(NH_2)_3$ is about 124 kJ mol^{-1} stronger than that to $Ta(NH_2)_3$.[21] The same is also applicable for coordination of CS. Our calculations show that the uptake of CS by $Re(NH_2)_3$ to form **5Re_S** is more exothermic than the uptake by $Ta(NH_2)_3$ to form **5Ta_T** (−376.5 kJ mol^{-1} for **5Re_S** versus −285.9 kJ mol^{-1} for **5Ta_T**, see Supporting Information). **5Ta_T**, having a triplet state, is calculated to be about 31.8 kJ mol^{-1} more stable than **5Ta_S**, having a singlet state (Figures 10 and 11). Ligands such as CS and CO, having two π^* orbitals, are capable of stabilizing both of the doubly occupied metal orbitals (d_{xz} and d_{yz}) of $Re(NH_2)_3$ and provide optimal metal−ligand interaction. In contrast, $Ta(NH_2)_3$, with the electron configuration d^2, cannot interact sufficiently with the double-face π-accepting ligands (CO and CS), giving the relatively weaker $(NH_2)_3$-Ta−CS and $(NH_2)_3Ta-CO$ bonds. The higher stability of **5Ta_T** versus **5Ta_S** (Figures 10 and 11) is likely a result of the fact that, in the former, both of the singly occupied d_π orbitals are stabilized by interaction with CS, while in the latter, only one of the d_π orbitals is stabilized (being doubly occupied). In comparison, CS_2, being mainly a single-face π-acceptor ligand, can only interact with one of the metal d_π orbitals.[49] The HOMO of the singlet state of $Ta(NH_2)_3$, lying 0.41 eV higher in energy than the HOMO of the singlet state of $Re(NH_2)_3$, is more prone to interact with CS_2. Since $Ta(NH_2)_3$ is a better donor, the Ta−CS_2 bond is stronger than the Re−CS_2 bond. **2Ta_T** is less stable than **2Ta_S** because, among the two metal d_π electrons, only one of them is mainly involved in interaction with CS_2.

After the π-complexes are formed, $(NH_2)_3M-CS_2$ (M = Ta or Re) coordinates to either $Re(NH_2)_3$ with triplet state or $Ta(NH_2)_3$ with singlet state through both of the sulfur atoms, lowering the energy of the systems by −296.1, −151.9, −239.9, and −98.7 kJ mol^{-1} for **3ReTa_S**, **3ReRe_T**, **3TaTa_S**, and

(49) Sakaki, S.; Tsuru, N.; Ohkubo, K. *J. Phys. Chem.* **1980**, *84*, 3390.

Table 1. Most Stable Spin State, Selected Calculated Structural Parameters (Bonds in Å), and Mulliken Partial Charges *q* of **I**

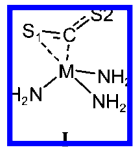

M	multiplicity	C−S1	C−S2	M−C	M−S1	q_{CS_2}
Re	singlet	1.733	1.634	1.949	2.428	−0.45
Ta	singlet	1.709	1.636	2.104	2.535	−0.52

Table 2. Most Stable Spin State, Selected Calculated Structural Parameters (Bonds in Å), and Mulliken Partial Charges *q* of **II**

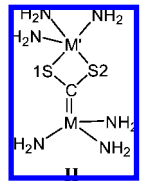

M	M′	multiplicity	C−S1	C−S2	M−C	M′−S1	M′−S2	q_{CS_2}	$q_{M(NH_2)_3}$	$q_{M'(NH_2)_3}$
Re	Ta	singlet	1.829	1.814	1.866	2.482	2.479	−0.53	+0.32	+0.21
Re	Re	singlet	1.822	1.837	1.867	2.369	2.331	−0.30	+0.36	−0.06
Ta	Ta	singlet	1.835	1.766	1.956	2.497	2.469	−0.59	+0.40	+0.19
Ta	Re	singlet	1.812	1.755	1.969	2.411	2.354	−0.35	+0.47	−0.12

Table 3. Most Stable Spin State, Selected Calculated Structural Parameters (Bonds in Å), and Mulliken Partial Charges *q* of **III**

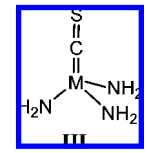

M	multiplicity	C−S	M−C	q_{CS}
Re	singlet	1.600	1.778	−0.34
Ta	triplet	1.598	1.966	−0.43

Table 4. Most Stable Spin State, Selected Calculated Structural Parameters (Bonds in Å), and Mulliken Partial Charges *q* of **IV**

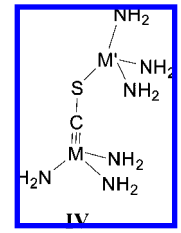

M	M′	multiplicity	C−S	M−C	M′−S	q_{CS_2}	$q_{M(NH_2)_3}$	$q_{M'(NH_2)_3}$
Re	Re	singlet	1.650	1.771	2.445	−0.19	+0.35	−0.16
Ta	Ta	singlet	1.644	1.886	2.237	−0.58	+0.21	+0.37
Ta	Re	singlet	1.636	1.911	2.204	−0.28	+0.30	−0.02

3TaRe_T, respectively. Our calculations show that the ground states of all the dinuclear intermediates are singlet. Therefore, it is expected that the triplet intermediates **3ReRe_T** (Figure 9) and **3TaRe_T** (Figure 11) require a spin crossover to be converted into the thermodynamically more stable singlet states. While a tetrahedral coordination around M is observed in the dinuclear intermediates $[(NH_2)_3M{-}CS_2{-}M'(NH_2)_3]$, the coordination around M′ is described as trigonal-bipyramidal, with an NH_2 group and a sulfur atom situated in the two axial positions. It is also worth noting that the formation of such a coordination of CS_2 has been earlier well established experimentally for other metal fragments.[13] Both of the C−S bonds are significantly elongated upon coordination of $(NH_2)_3MCS_2$ to $M'(NH_2)_3$, as shown from the comparison of C−S bond distances given in Tables 1 and 2. This result shows that the C−S bonds are more activated by $M'(NH_2)_3$ coordinating to $(NH_2)_3MCS_2$. The C−S bonds in the dinuclear intermediates are almost the same length as the C−S single bond (1.179 Å) calculated for $H_2C{=}C(SH)_2$. Thus, the Lewis structure **II** seems to be a very good model for the bonding description in these compounds. An analysis of the Mulliken charge distribution reveals that $M(NH_2)_3$ in the dinuclear intermediates is more positively charged than $M'(NH_2)_3$. It follows that the charge flow is mainly in the direction from $M(NH_2)_3$ to CS_2. The charge on $M'(NH_2)_3$ depends on the nature of the M′ metal center. The $M'(NH_2)_3$ metal fragments with M′ = Re carry a very small negative charge, while those with M′ = Ta are positively charged. This indicates that the ionic character in the Ta−S bonds of the compounds is higher than in the Re−S bonds. Indeed, the larger propensity of Ta to have a formal oxidation state +V enhances the ionic character of the Ta−S bond.

In the next step, the cleavage of the C−S bond of CS_2 takes place through the transition structures **1MM′_TS_S**, with energetic barriers of 0.5 and 20.2 kJ mol^{-1} for the **3ReTa_S** → **4Ta** + **5Re_S** (Figure 8) and **3ReRe_S** → **4Re** + **5Re_S** (Figure 9) reactions, respectively. We were unable to locate the transition structures connecting **3TaTa_S** to **4Ta** and **5Ta_S** (Figure 10), as well as **3TaRe_S** to **4Re** and **5Ta_S** (Figure 11), due to the flatness of the PES near the transition states. The cleavage process is exothermic for the **3ReTa_S** → **4Ta** + **5Re_S** (Figure 8) and **3ReRe_S** → **4Re** + **5Re_S** (Figure 9) reactions but is endothermic for the **3TaTa_S** → **4Ta** + **5Ta_S** (Figure 10) and **3TaRe_S** → **4Re** + **5Ta_S** (Figure 11) reactions. **5Ta_S**, derived from the cleavage process, is not stable and is subsequently converted to the more stable triplet analogue, **5Ta_T**, via an intersystem crossing process (Figures 10 and 11). These results indicate that CS_2 cleavage through only the $[(NH_2)_3Re/CS_2/Ta(NH_2)_3]$ and $[(NH_2)_3Re/CS_2/Re(NH_2)_3]$ systems would be energetically favorable.

Activation of CS. After cleavage of CS_2, both CS complexes **5Ta_T** and **5Re_S** are capable of binding to either $Re(NH_2)_3$, with triplet state, or $Ta(NH_2)_3$, with singlet state, to form the intermediate dimer complexes $[(NH_2)_3M{-}CS{-}M'(NH_2)_3]$. All attempts to optimize the intermediate $[(NH_2)_3Re{-}CS{-}Ta(NH_2)_3]$ led to CS cleavage and the direct formation of $(NH_2)_3ReC$ (**7Re**) and $(NH_2)_3TaS$ (**4Ta**) (Figure 8). This step, which is extremely exothermic, lends further support to the above proposal that $[N(R)Ar]_3Re/CS/Ta[N(R)Ar]_3$ is the best candidate for cleaving CS. The reaction of **5Re_S** with $Re(NH_2)_3$ gives $[(NH_2)_3Re{-}CS{-}Re(NH_2)_3]$ with a singlet ground state (**6ReRe_S**), preceded by a crossover from the triplet surface to the singlet surface (Figure 9). **6ReRe_S** is 41.6 kJ mol^{-1} lower in energy than its triplet analogue (**6ReRe_T**). Starting from **6ReRe_S**, the next step is CS cleavage, leading to the formation of $(NH_2)_3ReC$ (**7Re**) and $(NH_2)_3ReS$ (**4Re**). This step is calculated to be 30.5 kJ mol^{-1} exothermic and occurs via transition structure **2ReRe_TS_S**, with an activation barrier of 34.0 kJ mol^{-1}. Hence, it appears that CS cleavage through the $(NH_2)_3Re/CS/Re(NH_2)_3$ system is thermodynamically and kinetically viable. However, comparing the two energy profiles shown in Figures 8 and 9, one may conclude that cleavage of

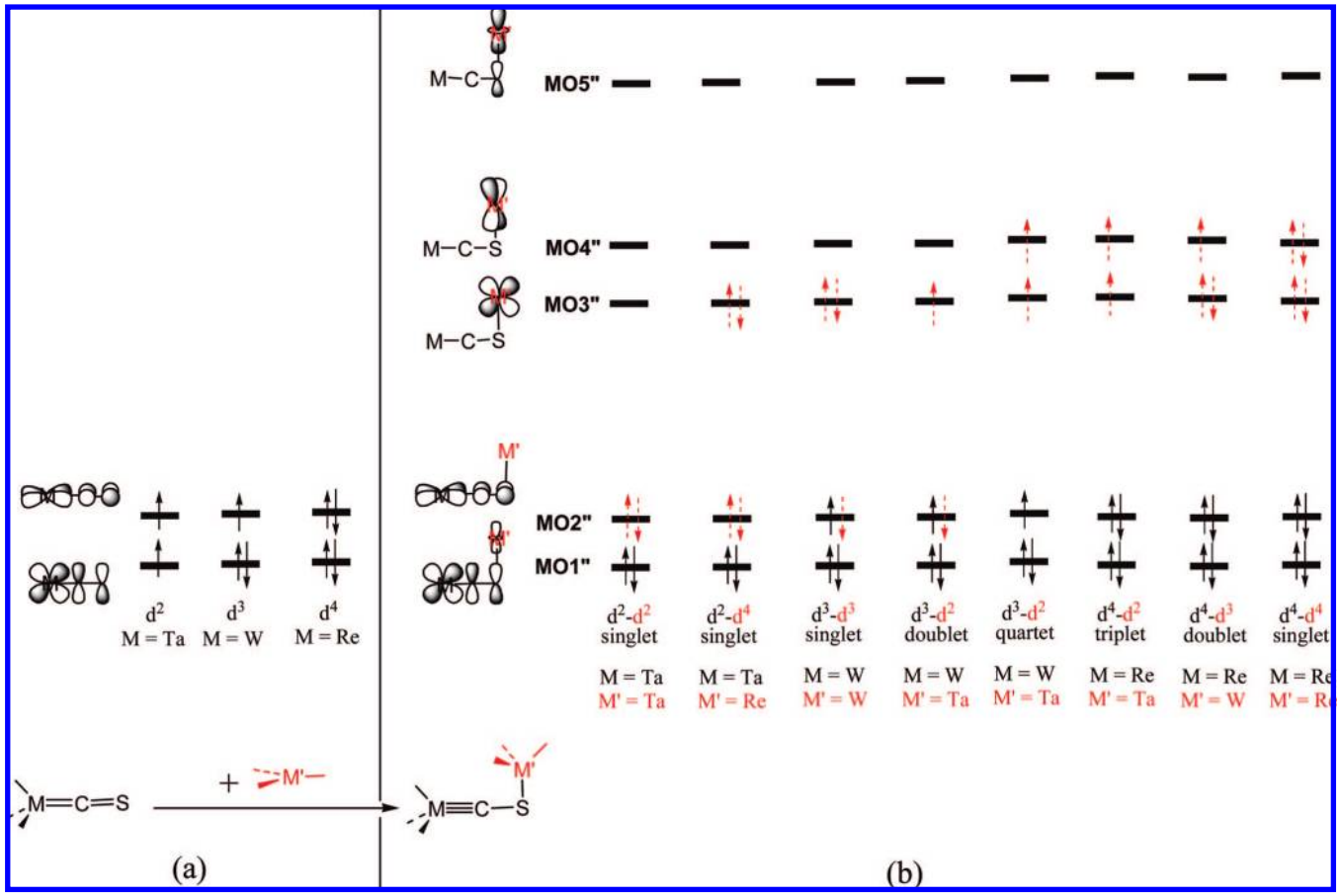

Figure 12. Molecular orbital diagram for the coordination of $M'(NH_2)_3$ to $(NH_2)_3M{=}C{=}S$.

both of the C−S bonds of CS_2 by the $[(NH_2)_3Re/CS_2/Ta(NH_2)_3]$ system is superior to that by the $[(NH_2)_3Re/CS_2/Re(NH_2)_3]$ system.

Our calculations also predict that the $[(NH_2)_3Ta{-}CS{-}Ta(NH_2)_3]$ and $[(NH_2)_3Ta{-}CS{-}Re(NH_2)_3]$ intermediates should be formed by the treatment of **5Ta-T** with $Ta(NH_2)_3$ and **5Ta-T** with $Re(NH_2)_3$, respectively (Figures 10 and 11). Both reactions are calculated to be exothermic. Starting from **6TaTa_S** and **6TaRe_S**, the CS cleavage step is endothermic by 157.4 kJ mol^{-1} for **6TaTa_S** → **4Ta** + **7Ta_T** and 256.4 kJ mol^{-1} for **6TaRe_S** → **4Re** + **7Ta_T**. Thus, C−S bond cleavage by these two metal systems is unlikely to occur, although both are capable of activating the C−S bonds (Tables 3 and 4). The C−S bond distances in **6TaTa_S** and **6TaRe_S** are lengthened when compared to those in **5Re_S** and **5Ta_T**. Regardless of what M is, the charge carried by the $M(NH_2)_3$ fragment is positive, suggesting that the metal-to-CS back-donation is mainly in the direction M → CS.

Other Possible Candidates for Activation of CS_2. For the sake of completeness, we also extended our calculations to other logical metal combinations such as $[NH_2]_3W/CS_2/W[NH_2]_3$, $[NH_2]_3W/CS_2/Ta[NH_2]_3$, $[NH_2]_3Re/CS_2/Nb[NH_2]_3$, and $[NH_2]_3Re/CS_2/W[NH_2]_3$ in order to show whether these newly designed systems are capable of cleaving CS_2. From the energy profiles shown in Figures A−D in the Supporting Information, one can easily find that, although all these four systems are able to cleave CS_2, only the $[NH_2]_3Re/CS_2/W[NH_2]_3$ and $[NH_2]_3Re/CS_2/Nb[NH_2]_3$ systems are feasible candidates for breaking of CS.

Comparing the energy profiles shown in Figures 1, 8–11, and A−D, one can find that the breaking of CS is possible only if the mixed-metal systems $[NH_2]_3Re/CS/M'[NH_2]_3$ (M′ = Nb, Ta, W, Re) are considered. In other words, of the mixed-metal systems studied in this work, those involving the d^4 Re^{III} center bound to C and the d^n M^{III} centers (n = 2, 3, and 4) bound to S are thermodynamically suited for cleaving CS. This behavior can be mainly attributed to the fact that $[NH_2]_3MCS + [NH_2]_3M'$ → $[NH_2]_3M{-}CS{-}M'[NH_2]_3$ is a moderately exothermic reaction when M = Re, while the same reaction is extremely exothermic when M = Mo, W, and Ta. Indeed, the dinuclear intermediate $[N(R)Ar]_3MCSM'[N(R)Ar]$ (M = Mo, W, and Ta) serves as a thermodynamic sink from which it is infeasible to reach $[N(R)Ar]_3MC$ and $[N(R)Ar]M'S$. For example, although the CS cleavage reaction $[NH_2]_3WCS + [NH_2]_3Ta$ → $[NH_2]_3TaS + [NH_2]_3WC$ (Figure B) is exothermic (125.1 kJ mol^{-1}), the much higher stability of **6WTa_D** relative to $[NH_2]_3TaS + [NH_2]_3WC$ (116.5 kJ mol^{-1}) is a crucial obstacle to the cleavage process.

To understand the reason behind this, let us again consider the molecular orbital interactions in such systems. Figure 12 shows the frontier orbitals for $[NH_2]_3MCS$ and $[NH_2]_3M{-}CS{-}M'[NH_2]_3$. In the HOMO and HOMO−1 of $[NH_2]_3MCS$, the metal(d)-to-CS(π^*) back-bonding interaction can be seen (Figure 12a). For M = Ta (d^2) and W (d^3), these two π orbitals are partially occupied, while for M = Re (d^4), these orbitals are fully occupied (Figure 12a). On the other hand, the d_π orbitals of $M'[NH_2]_3$ in $[NH_2]_3M{-}CS{-}M'[NH_2]_3$ essentially remain nonbonding because the metal-to-CS back-donation is in the direction from M to CS (Figure 12b). Once $[NH_2]_3Ta{-}CS{-}M'[NH_2]_3$ has formed, two electrons from $M'[NH_2]_3$ are transferred to the π-bonding orbitals of **MO1″**

and **MO2″** (Figure 12b), increasingly enhancing the stability of the dinuclear intermediate relative to $[NH_2]_3TaCS + [NH_2]_3M'$. A similar explanation can also be applicable for the stability of $[NH_2]_3W-CS-M'[NH_2]_3$ relative to $[NH_2]_3WCS + M'[NH_2]_3$, where the only difference is that one electron from $M'[NH_2]_3$ is involved in the π-bonding interactions. In contrast, for the case of $[NH_2]_3Re-CS-M'[NH_2]_3$, all the valence electrons of $M'[NH_2]_3$ should be accommodated in the nonbonding orbitals **MO3″** and **MO4″** or the σ antibonding orbital **MO5″**. In such a case, the expected bonding interaction does not happen, and the stability of $[NH_2]_3Re-CS-M'[NH_2]_3$ relative to $[NH_2]_3ReCS + M'[NH_2]_3$ remains comparable. This argument finds further support from comparison of the energy difference between **6WTa_D** and **6WTa_Q** (see Supporting Information). **6WTa_D** lies 241.6 kJ mol^{-1} below **5W** + $Ta[NH_2]_3$, while **6WTa_Q** has a stability comparable to that of the same reactants (Figure B, Supporting Information). This difference comes from the fact that one of the d electrons of $Ta[NH_2]_3$ is involved in the bonding interactions of **6WTa_D**, whereas in **6WTa_Q**, both d electrons of $Ta[NH_2]_3$ occupy the nonbonding orbitals **MO3″** and **MO4″** (Figure 12b).

Conclusions

The overall mechanism for the activation of CS_2 is seen to follow this sequence: initial binding of the carbon of the CS_2 molecule to the metal fragment ML_3, binding of a second (possibly different) metal fragment $M'L_3$ to bridge the two sulfur atoms, breaking of a C−S bond and formation of L_3M-CS and $L_3M'S$, and finally binding of a third metal fragment M'_3 to the sulfur of CS,which may or may not lead to breaking of the second C−S bond. When $M = M' =$ Mo, our theoretical results show that breaking the second C−S bond is endothermic by about 200 kJ mol^{-1}, and so the reaction stops after breaking only the first C−S bond. This is in perfect agreement with experimental findings and can be understood in terms of the relative strengths of the Mo−C, Mo−S, and C−S bonds.

We have investigated further the nature of the M−S bond. We have shown that the bond strength can be rationalized in terms of the interaction between the metal d and sulfur p orbitals and the occupancy of the resulting π^* molecular orbital. The M−S bond strength can also be understood in terms of the change in oxidation of the metal. On both counts, Ta is shown to be the metal of choice for forming bonds with sulfur.

Given the above information on the M−S bond and our previous results indicating that Re forms a strong bond with carbon, it comes as no surprise, perhaps, that our conclusion from this paper is that the mixed-metal system $L_3Re/CS_2/TaL_3$ should provide the best possibility of the neutral ML_3 fragments cleaving both C−S bonds in CS_2. Not only are the barriers very small, but the overall exothermicity of 700 kJ mol^{-1} provides a very strong driving force for the reaction. The present work shows that the $L_3Re/CS_2/ReL_3$ system can also cleave both C−S bonds, and because of the lesser exothermicity of this reaction compared to that with a Re−Ta system, it may provide a better basis for developing a catalytic cycle. The $L_3Ta/CS_2/TaL_3$ and $L_3Ta/CS_2/ReL_3$ systems are predicted to be unsuitable for CS_2 activation, and the latter system may not even break the first C−S bond under experimental conditions.

Finally, when we turn our attention to the CS molecule by itself, it is clear that the mechanism for activation of CS follows, in very broad terms, that outlined previously for other diatomic molecules with multiple bonds (e.g., N_2). Although ML_3-activated cleavage of the C−S bond has not yet been observed experimentally, we have shown in this work that the $L_3Re-CS-TaL_3$ system is predicted to result in spontaneous C−S bond cleavage and that $L_3Re-CS-ReL_3$, while less dramatic, may also be a useful experimental system for the activation of CS.

This study has validated the use of simple M−X bond strength arguments in predicting which mixed-metal systems are most likely to be of use in activating multiple bonds in small molecules. This study also reinforces the crucial role that the early transition metal complexes play in the activation of such molecules.

Acknowledgment. The authors thank the Australian Research Council (ARC) for project funding and the University of Tasmania and the Australian Partnership for Advanced Computing (APAC) for generous grants of time at their high-performance computing facilities.

Supporting Information Available: Total energies and Cartesian coordinates of all structures, basis set information for the large basis set single-point calculations, potential energy surfaces for CS activation, and complete ref 33. This material is available free of charge via the Internet at http://pubs.acs.org.

JA800946E